apodized by a sine-bell function, zero-filled, and Fourier-transformed, and the absolute value was taken and symmetrized. The resolution was 1.75 Hz in each dimension. The data were plotted with a Zeta plotter. The total time for data processing and plotting was about 1 h.

Two-Dimensional ¹H–¹H J-Correlated Spectrum of 21. The data were acquired by using the UCB-200 NMR spectrometer (Cryomagnet Systems Inc. superconducting magnet operating on 201.9-MHz proton frequency, Nicolet 1180 computer, Nicolet 293A′ pulse programmer) and processed with a Nicolet 1180E computer. Nicolet's correlated spectrum (COSY) experiment was used to provide the pulse program. The 90° ¹H pulse was 7.7 μs. The fixed delay was 7.0 μs to emphasize couplings less than 35 Hz. The incremental delay was equal to the dwell time of 500 μs. The sweep width was 1000 Hz. The spectrometer frequency was set at the left edge of the spectrum, 5.3 ppm. Single-phase detection was used. The pulse delay was 2 s. When a 0.1 M solution of **21** in C_6D_6 was scanned, 16 1K transients were collected for each of the 256 incremental spectra. The total time for data acquisition was less than 3 h. The data were apodized by a sine-bell function and Fourier-transformed. After transposing the matrix, the data were apodized by a sine-bell function, zero-filled, and Fourier-transformed, and the absolute value was taken and symmetrized. The resolution was 1.95 Hz in both dimensions. The data were plotted with a Zeta plotter. The total time for data processing and plotting was about 1 h.

Two-Dimensional ¹³C–¹H Chemical Shift Correlation Map of 21. The data were acquired by using the UCB-250 NMR spectrometer (Cryomagnet Systems Inc. superconducting magnet operating on 250.8-MHz proton frequency, Nicolet 1180 computer, Nicolet 293A′ pulse programmer) and processed with a Nicolet 1180E computer. Nicolet's chemical shift correlation map (CSCM) experiment was used to provide the pulse program. The 90° ¹H pulse from the decoupler was 36 μs. The 180° ¹³C pulse was 37 μs. The two fixed delays were 3.0 and 2.5 ms. The incremental mixing delay was 227 μs to give a proton spectral width of 4.4 ppm. Single-phase detection was used. The decoupler frequency

was set at the left edge of the proton spectrum at 4.9 ppm. The spectrometer frequency was set at the left edge of the carbon region, 103 ppm. The sweep width was 88 ppm. The pulse delay was 1.3 s. When a 0.5 M solution of **21** in C_6D_6 was scanned, 72 4K transients were collected for each of the 256 incremental spectra. The total time for data acquisition was 7.5 h. The data were apodized by a sine-bell function and Fourier-transformed in the carbon dimension. After the matrix was transposed to the proton dimension, the data were apodized by a sine-bell function, zero-filled, and Fourier-transformed, and the absolute value was taken. The resolution was 1.4 Hz in the carbon dimension and 2.2 Hz in the proton dimension. The data were plotted with a Zeta plotter. The total time for data processing and plotting was about 2 h.

Registry No. 4, 94732-58-8; **5,** 94732-59-9; **6,** 94732-60-2; **7,** 87226-59-3; **8,** 87226-60-6; **9,** 94732-61-3; **10,** 94732-62-4; **11,** 94732-63-5; **12,** 94751-08-3; **13,** 94732-64-6; **14,** 94732-65-7; **15,** 94732-66-8; **16,** 94751-09-4; **17,** 94732-67-9; **18,** 94732-68-0; **19,** 94732-69-1; **20,** 94751-10-7; **21,** 94751-11-8; **22,** 94732-70-4; **23,** 94751-12-9; **24,** 94732-71-5; **25,** 94751-13-0; **26,** 94732-72-6; **27,** 94751-14-1; CpCo-(CO)₂, 12078-25-0; (CH₃)₃SiCH₂MgCl, 13170-43-9; 1,6-heptadiyne, 2396-63-6; 3-bromopropanal ethylene acetal, 18742-02-4; 4-bromo-1-butene, 5162-44-7; 1,7-octadiyne, 871-84-1; (chloromethyl)trimethylsilane, 2344-80-1; methyl-d₃-triphenylphosphonium iodide, 1560-56-1.

Reaction of the Samarium–Hydrogen Bond in [(C₅Me₅)₂SmH]₂ with Carbon Monoxide: Formation, Isomerization, and X-ray Crystallographic Characterization of cis- and trans-{(C₅Me₅)₂[(C₆H₅)₃PO]Sm}₂(μ-OCH=CHO)[1,2]

William J. Evans,[3] **Jay W. Grate, and Robert J. Doedens**

Contribution from the Department of Chemistry, University of California, Irvine, California 92717. Received July 30, 1984

Abstract: [(C₅Me₅)₂SmH]₂ (I) reacts with CO in arene solvents to form a product, II, which generates crystals of cis-{(C₅Me₅)₂[(C₆H₅)₃PO]Sm}₂(μ-OCH=CHO) (IIIa) when (C₆H₅)₃PO is added. IIIa crystallizes from toluene under hexane diffusion in space group P1̄ with unit cell dimensions *a* = 18.673 (7) Å, *b* = 17.641 (6) Å, *c* = 13.973 (5) Å, α = 102.40 (3)°, β = 93.57 (3)°, γ = 93.15 (3)°, and Z = 2 (with six toluene molecules of crystallization per unit cell) for D_c = 1.27 g cm⁻³. Least-squares refinement on the basis of 6427 observed reflections led to a final *R* value of 0.065. IIIa isomerizes to the trans isomer IIIb at room temperature in hours to days depending on sample concentration. IIIb crystallizes from toluene under hexane diffusion in space group P2₁/n with unit cell dimensions *a* = 14.678 (2) Å, *b* = 17.424 (3) Å, *c* = 28.736 (4) Å, β = 100.67 (1)°, and Z = 4 for D_c = 1.34 g cm⁻³. Least-squares refinement on the basis of 8312 observed reflections led to a final *R* value of 0.051. In both IIIa and IIIb, (C₅Me₅)₂Sm[OP(C₆H₅)₃] units are connected by a bridging —OCH=CHO— moiety. The two C₅Me₅ ring centroids, the OPPh₃ oxygen atom, and the enediolate oxygen atom describe a distorted tetrahedral coordination geometry around each samarium center. The enediolate bridge is best resolved in the cis isomer IIIa and has the following bond distances (Å): Sm—O, 2.147 (10) and 2.179 (10); C—O, 1.319 (19) and 1.352 (18); C=C, 1.324 (22). O—C=C angles of 132.51 (18)° and 128.4 (18)° were observed. In the trans isomer IIIb there is an apparent rotational disorder of the bridging group about the Sm—O bonds.

Carbon monoxide is one of the most extensively investigated ligands in organometallic chemistry. In recent years,, the desire to use CO as a feedstock has encouraged research on both the homogeneous and heterogeneous conversion of CO/H₂ mixtures

("syn-gas") to reduced, homologated oxygenates and hydrocarbons.[4–12] One reaction that has been studied to model hydrogen

---

(1) Part 7 of the series Organolanthanide and Organoyttrium Hydride Chemistry. Part 6: Evans, W. J.; Meadows, J. H.; Hanusa, T. P. *J. Am. Chem. Soc.* **1974**, *106*, 4454–4460.
(2) Presented in part at the Industrial Associates Conference on Recent Trends in Heterogeneous and Homogeneous Catalysis, California Institute of Technology, March 21–23, 1984.

(3) Alfred P. Sloan Research Fellow.
(4) Ponec, V. *Catal. Rev.—Sci. Eng.* **1978**, *18*, 151–171.
(5) Masters, C. *Adv. Organomet. Chem.* **1979**, *17*, 61–103 and references therein.
(6) Kung, H. H. *Catal. Rev.—Sci. Eng.* **1980**, *22*, 235–259.
(7) Klier, K. *Adv. Cat.* **1982**, 243–313.
(8) Dombek, B. D. *Adv. Cat.* **1983**, *32*, 325–416 and references therein.
(9) Muetterties, E. L.; Stein, J. *Chem. Rev.* **1979**, *79*, 479–490.

reduction of CO is the reaction of a metal hydride with CO to form a formyl complex[12] (eq 1). The formation of metal formyl

$$MH + CO \rightarrow MC(=O)H \qquad (1)$$
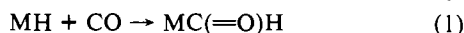
complexes by this route has been synthetically difficult because thermodynamic considerations generally favor the reverse reaction, namely, decarbonylation of the formyl to CO and a metal hydride.[12-14] Oxophilic metals, such as the early transition metals, lanthanides, and actinides can be used to advantage in this regard, since intermediate formyls can be stabilized by coordination of both C and O to the metal center.

$$MC(=O)H - M\overset{\longleftarrow}{}:CO—H$$

Indeed, hydrides of early transition metals have displayed an extensive chemistry with CO[10,11,13,15,16] and actinide hydrides react rapidly with CO to give spectroscopically observed η^2-formyl complexes at low temperature.[17]

Our previous studies of the reaction of CO with $(C_5H_5)_2Lu$-$(t\text{-}C_4H_9)(THF)$ to form $(C_5H_5)_2Lu(COCMe_3)$ and $[(C_5H_5)_2Lu]_2(CO)_4(CMe_3)_2$ (eq 2; $Cp = C_5H_5$, $R = CMe_3)$[18] as

$$2Cp_2LuR(THF) + 2CO \longrightarrow 2Cp_2LuCR \overset{O}{\underset{|}{\parallel}} \overset{2CO}{\longrightarrow} \quad (2)$$
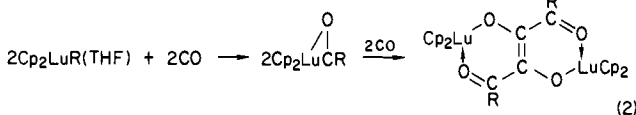
well as the observed reaction of CO with $(C_5Me_5)_2Sm(THF)_2$[19] indicated that organolanthanide complexes display interesting chemistry with CO. Reactions of organometallic lanthanide hydrides and CO have not previously been reported primarily because molecular lanthanide hydride complexes were not known until recently.[20,21] We now have a variety of well-characterized organolanthanide and organoyttrium hydrides in hand, including $[(C_5H_4R)_2Ln(THF)(\mu\text{-}H)]_2$[22] (R = H, CH_3; Ln = Tb, Er, Lu, Y), $[(C_5Me_5)_2SmH]_2$,[23] $[(C_5H_5)_2ErH]_3Cl^-$,[24] $[(C_5H_5)_2LnH]_3H^-$ (Ln = Y, Er, Lu),[1,24,25] and $\{[(CH_3C_5H_4)_2YH]_2[(CH_3C_5H_4)_2$-$ZrH]H\}$,[1] and have begun a study of their reactivity with CO.

In this report we describe the rapid reaction of $[(C_5Me_5)_2SmH]_2$ with CO to generate a product which can be isolated as a triphenylphosphine oxide (TPPO) adduct. In this system, carbon monoxide is both reduced and dimerized to yield a bridging enediolate ligand with cis geometry. We describe here the synthesis of this complex, the full details of its structure determined by X-ray crystallography, the isomerization of the cis enediolate ligand to the trans isomer, and the characterization of the trans isomer by X-ray crystallography. These studies have provided the first direct structural information on an unsubstituted enediolate ligand

derived from carbon monoxide and a metal hydride. In addition, the isomerization of the cis enediolate bridge is a reaction with little precedent in the literature.

Experimental Section

The complexes described below are extremely air and moisture sensitive. Therefore, both the syntheses and subsequent manipulations of these compounds were conducted under nitrogen with rigorous exclusion of air and water using Schlenk, vacuum line, and glovebox (Vacuum/Atmospheres HE-553 Dri Lab) techniques.

Materials. Hexane was washed with sulfuric acid, dried over $MgSO_4$, and distilled from potassium benzophenone ketyl solubilized with tetraglyme. Toluene and THF were distilled from potassium benzophenone ketyl. Benzene, THF-d_8, benzene-d_6, and toluene-d_8 were vacuum transferred from potassium benzophenone ketyl. CO (99.99%, Liquid Carbonic) and triphenylphosphine oxide (Aldrich) were used as received. $(C_5Me_5)_2Sm(THF)_2$ was prepared from SmI_2 and KC_5Me_5.[26] $[(C_5Me_5)_2SmH]_2$ (I) was prepared from $(C_5Me_5)_2Sm(THF)_2$, diphenylacetylene, and H_2 as described in ref 23. However, the product was collected as the precipitate from the hydrogenolysis reaction in alkane solvent, rinsed with alkane, and dried in vacuo. It was not exposed to arenes, with which it reacts slowly (over days), until it was used. Powdered I isolated in this manner can be stored for weeks at -25 °C in a well-sealed vial in the glovebox.

Physical Measurements. Infrared spectra were obtained on a Perkin-Elmer 283 spectrometer as previously described.[21] ^{1}H NMR spectra were obtained on a Bruker WM-250 spectrometer at 295 K unless otherwise noted. Chemical shifts were assigned relative to C_6D_5H, 7.15 ppm, for spectra in benzene-d_6, or relative to $C_6D_5CD_2H$, 2.15 ppm, for spectra in toluene-d_8. Complete elemental analyses were obtained from Analytische Laboratorien, Engelskirchen, West Germany. Magnetic susceptibilities were determined by the Evans method on the 250-MHz spectrometer.[27]

Apparatus and Methods for the CO Reactions. Reactions were carried out in 3-oz Lab-Crest (Fischer-Porter) glass pressure reaction vessels. The stainless steel coupling to the glass vessel was equipped with a pressure-relief valve, a pressure gage, a bellows valve, and a VCO coupling. With the bellows valve closed, the contents of the reactor were sealed from the atmosphere. For NMR experiments, an NMR tube was loaded with a solution of $[(C_5Me_5)_2SmH]_2$ (I) in benzene-d_6 or toluene-d_8 and then placed inside the reaction vessel. For preparative reactions the solutions were loaded directly into the glass pressure vessel and a Teflon stir bar was added. The reactor was sealed and placed on a metal vacuum line via the VCO coupling. Carbon monoxide was delivered to the line via a Matheson high-purity regulator. The line, which was connected to a Schlenk line via a plug valve, could be vented via another plug valve and a bubbler and was equipped with a pressure-relief valve. Before initiating a reaction, the metal vacuum line from the CO cylinder valve to the reactor bellows valve was purged of air by using the Schlenk line, evacuated, and pressurized to 90 psi CO. The bellows valve was then opened to pressurize the reaction. Nitrogen was removed from the reaction vessel by venting the line to 1 atm through the bubbler, repressuring, venting, etc. **CAUTION:** Glass pressure vessels should be protected with a wire mesh and a shield. Reaction of I with CO is essentially as rapid as mixing, based on the color change, but most reactions were left at 90 psi for 1–2 h. (Mixing in unstirred NMR tubes is slow.) Reaction also occurs at 1 atm, but reaction at 90 psi is rapid and convenient. When reactions were complete, the line was vented to 1 atm, the bellows valve was sealed, and the reactor under 1 atm of CO was returned to the glovebox for workup.

Initial Product of the $[(C_5Me_5)_2SmH]_2$/CO Reaction, II. In the glovebox, $[(C_5Me_5)_2SmH]_2$ (I) (0.175 g, 0.207 mmol) was dissolved in 10 mL of toluene to give an orange solution, which was placed in the glass pressure apparatus with a Teflon stir bar. The apparatus was attached to the metal vacuum line and pressurized to 90 psi with CO. The solution turned red-brown after CO was admitted and stirring began. After returning the solution to the glovebox, removal of the toluene left a tacky, red-brown solid which was dissolved in hexane. Removal of the hexane left a drier, glassy solid. IR spectra were run both as a KBr pellet and as a neat film deposited on a salt plate with hexane (which evaporated). These spectra were essentially identical, and in each case, the base-line rose to medium intensity from 1660 to 900 cm^{-1}, capped with peaks from 1580 to 980 cm^{-1}. IR (neat) 2955 (s), 2906 (s), 2858 (s), 1589 (w), 1563 (w), 1544 (m), 1530 (m), 1492 (m), 1436 (s), 1378 (m), 1267 (m), 1228 (m), 1187 (m), 1160 (m), 1134 (m), 1110 (m), 1018 (m), 981 (m), 810

(10) Bercaw, J. E.; Wolczanski, P. T. *Acc. Chem. Res.* **1980**, *13*, 121–127 and references therein.

(11) Erker, G. *Acc. Chem. Res.* **1984**, *17*, 103–109 and references therein.

(12) Gladysz, J. A. *Adv. Organomet. Chem.* **1982**, *20*, 1–38 and references therein.

(13) Manriquez, J. M.; McAlister, D. R.; Sanner, R. D.; Bercaw, J. E. *J. Am. Chem. Soc.* **1978**, *100*, 2716–2724.

(14) But see: Wayland, B. B.; Woods, B. A. *J. Chem. Soc., Chem. Commun.* **1981**, 700–701. Wayland, B. B.; Woods, B. A.; Pierce, R. *J. Am. Chem. Soc.* **1982**, *104*, 302–303.

(15) Fachinetti, G.; Floriani, C.; Roselli, A.; Pucci, S. *J. Chem. Soc., Chem. Commun.* **1978**, 269–270.

(16) Gell, K. I.; Schwartz, J. *J. Organomet. Chem.* **1978**, *162*, C11–C15.

(17) Fagan, P. J.; Moloy, K. G.; Marks, T. J. *J. Am. Chem. Soc.* **1981**, *103*, 6959–6962 and references therein.

(18) Evans, W. J.; Wayda, A. L.; Hunter, W. E.; Atwood, J. L. *J. Chem. Soc., Chem. Commun.* **1981**, 706–708.

(19) Evans, W. J.; Bloom, I.; Hunter, W. E.; Atwood, J. L. *J. Am. Chem. Soc.* **1981**, *103*, 6507–6508. Evans, W. J.; Grate, J. W.; Hughes, L. A.; Zhang, H.; Atwood, J. L., submitted for publication.

(20) Evans, W. J. *Adv. Organomet. Chem.*, in press, and references therein.

(21) Evans, W. J.; Meadows, J. H.; Hunter, W. E.; Atwood, J. L. *J. Am. Chem. Soc.* **1984**, *106*, 1291–1300 and references therein.

(22) Evans, W. J.; Meadows, J. H.; Wayda, A. L.; Hunter, W. E.; Atwood, J. L. *J. M. Chem. Soc.* **1982**, *104*, 2008–2014.

(23) Evans, W. J.; Bloom, I.; Hunter, W. E.; Atwood, J. L. *J. Am. Chem. Soc.* **1983**, *105*, 1401–1403.

(24) Evans, W. J.; Meadows, J. H.; Wayda, A. L.; Hunter, W. E.; Atwood, J. L. *J. Am. Chem. Soc.* **1982**, *104*, 2015–2017.

(25) Evans, W. J.; Meadows, J. H., unpublished results.

(26) Evans, W. J.; Grate, J. W.; Bloom, I.; Choi, H. W.; Hunter, W. E.; Atwood, J. L. *J. Am. Chem. Soc.*, in press.

(27) Evans, D. F. *J. Chem. Soc.* **1959**, 2003–2005. Becconsall, J. K. *Mol. Phys.* **1968**, *15*, 129–139.

Reaction of the Samarium–H Bond in [(C$_5$Me$_5$)$_2$SmH]$_2$

J. Am. Chem. Soc., Vol. 107, No. 6, 1985 1673

Table I. Crystal Data and Summary of Intensity Data Collection and Structure Refinement for *cis*-{(C$_5$Me$_5$)$_2$[(C$_6$H$_5$)$_3$PO]Sm}$_2$(μ-OCH=CHO) (IIIa)

compd	Sm$_2$P$_2$C$_{78}$H$_{92}$O$_4$
M_r	1456.3
space group	$p\bar{1}$
cell constants	
a, Å	18.673 (7)
b, Å	17.641 (6)
c, Å	13.973 (5)
α, deg	102.40 (3)
β, deg	93.57 (3)
γ, deg	93.15 (3)
cell vol, Å^3	4476 (3)
molec/unit cell	2, 6 toluene
ρ(calcd), g cm^{-3}	1.27
μ(calcd), cm^{-1}	13.87
transmsn factor range	0.840–0.883
radiatn	Mo Kα λ = 0.710 73 Å graphite monochromator
max cryst dimens, mm	0.35 × 0.31 × 0.25
scan width	−1.2° in 2θ from Kα_1 to +1.2° from Kα_2
scan rate, deg min^{-1}	variable, 2–12 (2θ, 0–35°), 4–12 (2θ, 35–45°)
std reflcns	2,1,1 2,−1,1 −2,1,3
decay of std	16%, isotropic
reflcns measured	11758
2θ range	0–45°
obsd reflcns	6427 (>3σ)
bkgd counting	bkgds evaluated from 96-step peak profile
no. of params varied	595
GOF	2.25
R	0.065
R_w	0.087
temp	24 °C

Table II. Crystal Data and Summary of Intensity Data Collection and Structure Refinement for *trans*-{(C$_5$Me$_5$)$_2$[(C$_6$H$_5$)$_3$PO]Sm}$_2$(μ-OCH=CHO) (IIIb)

compd	Sm$_2$P$_2$C$_{78}$H$_{92}$O$_4$
M_r	1456.3
space group	$P2_1/n$
cell constants	
a, Å	14.678 (2)
b, Å	17.424 (3)
c, Å	28.736 (4)
β, deg	100.67 (1)
cell vol, Å^3	7222 (2)
molec/unit cell	4
ρ(calcd), g cm^{-3}	1.34
μ(calcd), cm^{-1}	17.10
transmsn factor range	0.716–0.742
radiatn	Mo Kα λ = 0.710 73 Å graphite monochromator
max cryst dimens, mm	0.42 × 0.54 × 0.51
scan width	−1.2° in 2θ from Kα_1 to +1.2° from Kα_2
scan rate, deg min^{-1}	variable, 4–12
std reflcns	0,−2,−2 2,0,0 2,0,−4
decay of std	7.0%, isotropic
reflcns measured	13799
2θ range	0–50°
obsd reflcns	8312 (>3σ)
bkgd counting	bkgd evaluated from 96-step peak profile
no. of params varied	523
GOF	2.29
R	0.051
R_w	0.085
temp	24 °C

(m) cm^{-1}; ^{1}H NMR (benzene-d_6) δ −0.7 (br, $w_{1/2}$ = 16 Hz) ppm. At 253 K the signal broadened to a half-width of approximately 250 Hz and at 233 K it disappeared into the base line. New signals began to appear at 223 K, and at 213 K the principle features of the spectrum were broad signals at 2.8 and −3.8 ppm, with two small broad satellites placed asymmetrically about the latter peak. At 193 K the satellites disappeared, and II had peaks at 3.0 (half-width = 20 Hz) and −3.5 ppm (half-width = 83 Hz) in a ratio of 3:7.

cis-{(C$_5$Me$_5$)$_2$[(C$_6$H$_5$)$_3$PO]Sm}$_2$(μ-OCH=CHO) (IIIa). In the glovebox, [(C$_5$Me$_5$)$_2$SmH]$_2$ (I) (0.182 g, 0.216 mmol) was dissolved in 10 mL of benzene to give an orange solution, which was placed in the glass pressure apparatus with a Teflon stir bar. The apparatus was attached to the metal vacuum line and pressurized to 90 psi with CO. The solution turned red-brown after CO was admitted and the stirring began. After returning the solution to the glovebox, triphenylphosphine oxide (0.243 g, 0.873 mmol) dissolved in 4 mL of benzene was added. Some of the product separated from solution as large orange crystals overnight. The crystals were collected, rinsed twice with benzene, pulverized with a spatula, and dried in vacuo (115 mg, 0.079 mmol, 37%). Anal. Calcd for SmC$_{39}$H$_{46}$PO$_2$: Sm, 20.65; C, 64.33; H, 6.37; P, 4.25; O, 4.39. Found: Sm, 20.90; C, 64.24; H, 6.35; P, 4.31; O (by difference), 4.20. ^{1}H NMR (benzene-d_6) δ 1.68 (s, C$_5$(CH$_3$)$_5$, 30 H), 10.70 (s, =CHO, 1 H), 6.83, 6.81 (overlapping broad singlets, (C$_6$H$_5$)$_3$PO, meta and para, 9 H), 6.01 (s, v br, (C$_6$H$_5$)$_3$PO, ortho, 6 H); IR (KBr) 3055 (w), 2890 (s), 2849 (s), 1600 (m), 1590 (m), 1480 (w), 1437 (s), 1400 (s), 1329 (w), 1153 (s), 1129 (s), 1087 (s), 1012 (m), 994 (m), 841 (s), 742 (m), 718 (s), 687 (s) cm^{-1}. Rotary evaporation of the mother liquor gave a residue that contained both IIIa and IIIb observed by NMR at 1.68 and 1.89 ppm, respectively.

Powdered IIIa was recrystallized in a vial by making a saturated solution in toluene, layering hexane over this, and allowing diffusion to occur at glovebox temperature (ca. 30 °C). The following day, both needles and polyhedra were present as described in the Results. A polyhedral crystal was selected from this mixture, mounted in a glass capillary in the glovebox, and analyzed by X-ray crystallography as described in the next section.

X-ray Data Collection, Structure Determination, and Refinement for IIIa. X-ray data were collected on a Syntex P2$_1$ diffractometer by procedures previously described.[28] Refined cell parameters were obtained from the settings of 15 reflections with 30° ≤ 2θ ≤ 35°. Interaxial angles

indicated triclinic symmetry, which was confirmed by a Delaunay reduction. The lower limit of the variable scan rate was increased after 2θ = 35° because of decay of standards, which were measured every 100 reflections. Data were collected by the θ–2θ scan technique in bisecting geometry. The *p* factor in the expression[29] for the standard deviation of the observed intensities was given a value of 0.05. Crystal data and experimental parameters are summarized in Table I.

All computations were carried out with a local version of the UCLA Crystallographic Computing Package.[30] The space group $P\bar{1}$ was indicated by intensity statistics and was confirmed by the successful solution and refinement of the structure. Data collection was terminated at 2θ = 45° because only a small fraction (<10%) of intensities beyond this point were above background. Data were corrected for Lorentz, polarization, and absorption effects and for decay of standards.

Solution of the structure was achieved by Patterson and difference Fourier methods. Refinement was carried out with the triphenylphosphine oxide phenyl rings as rigid groups, isotropic thermal parameters for the group atoms and for the toluene atoms, and an isotropic temperature factors for all other atoms. Hydrogen atoms were not located. In all structure factor calculations, atomic scattering factors were taken from ref 31. A final difference Fourier map revealed no anomalous features and a maximum peak height of 1.16 e Å^{-3}. In the final refinement cycle, the parameter shifts of all atoms except some of the toluene carbon atoms were less than 0.10 of their standard deviations.

trans-{(C$_5$Me$_5$)$_2$[(C$_6$H$_5$)$_3$PO]Sm}$_2$(μ-OCH=CHO) (IIIb). Crystals from the recrystallization of powdered IIIa were redissolved in excess toluene, hexane was layered above the toluene, and diffusion proceeded at box temperature. Crystals did not appear until a few days later, growing to large needles. The mother liquor was poured off and the crystals were dried in the glovebox atmosphere. ^{1}H NMR (benzene-d_6) δ 1.89 (s, C$_5$(CH$_3$)$_5$, 30 H), 11.44 (s, =CHO, 1 H), 6.74–6.37 (overlapping multiplets, (C$_6$H$_5$)$_3$PO, meta and para, 9 H), 6.04 (s, v br, (C$_5$H$_5$)$_3$PO, ortho 6 H); IR (KBr) 3058 (w), 2905 (s), 2858 (s), 1592 (w), 1487 (w), 1440 (s), 1377 (w), 1283 (m), 1184 (s), 1152 (s), 1120 (s), 1089 (s), 1028 (m), 997 (m), 874 (w), 746 (m), 718 (s), 689 (s) cm^{-1}; $\chi_M^{295 K}$ = 1500 × 10^{-6}, μ_{eff} = 1.9 μ_B. A single needle was cleaved in to smaller sections with a razor blade and mounted under nitrogen in a glass capillary for examination by X-ray crystallography as described in the next section.

X-ray Data Collection, Structure Determination, and Refinement for IIIb. Data collection and refinement were carried out by the methods

(28) Sams, D. B.; Doedens, R. J. *Inorg. Chem.* 1979, *18*, 153–156.

(29) Corfield, P. W. R.; Doedens, R. J.; Ibers, J. A. *Inorg. Chem.* 1967, *6*, 197–204.

(30) Strouse, C. E., personal communication to R. J. Doedens.

(31) "International Tables for X-ray Crystallography"; Kynoch Press: Birmingham, England, 1974; Vol. IV, p 72.

described above for IIIa. Crystal data and experimental parameters are summarized in Table II. Refined cell parameters were obtained from the settings of 15 reflections with $30° \leq 2\theta \leq 35°$. Monoclinic symmetry was indicated by the interaxial angles and confirmed by axial rotation photography. The space group $P2_1/n$ was uniquely determined by the systematic absences, $h0l$, $h + l \neq 2n$, and $0k0$, $k \neq 2n$. Data collection was terminated at $2\theta = 45°$ because only a small fraction (<10%) of intensities beyond this point were above background. Data were corrected for Lorentz, polarization, and absorption effects and for standard decay.

Solution of the structure was achieved by Patterson and difference Fourier methods. Isotropic refinement of all non-hydrogen atoms led to $R = 0.071$ and $R_w = 0.104$, but the carbon–carbon bond distance of the bridging enediolate ligand was unreasonably short at 1.07 Å. These two atoms were therefore removed, the phenyl rings were refined as rigid groups, and the remaining atoms were refined anisotropically. After refinement to $R = 0.071$ and $R_w = 0.107$, a difference Fourier map revealed three peaks in the region of the carbons of the enediolate bridge. The two giving the best C–C bond distance and C–C–O angles were assigned as carbon atoms and refined anisotropically. Convergence at $R = 0.052$ and $R_w = 0.085$ led to a bridge carbon–carbon bond distance of only 0.97 Å. A difference Fourier map showed one peak near the bridge which gave a more reasonable C–C bond distance, so it was assigned as a carbon atom in place of one of the bridge carbon atoms. However, on subsequent refinement, the bridge C–C bond distance shortened again. Because there was no well-defined alternative model for the bridging group, refinement was terminated at this point.

The final convergence led to $R = 0.051$ and $R_w = 0.085$ and a bridge carbon–carbon bond distance of 0.96 (2) Å. A final difference map gave a maximum peak height of 1.05 e Å^{-3}, and in the final refinement, the parameter shifts of all atoms except the bridge carbons were less than 0.26 of their standard deviations. The unreasonably short bridge carbon–carbon bond distance and large temperature factors for these atoms led to the conclusion that these atoms are disordered. The conclusion that this enediolate bridge is trans is supported by examination of drawings of the structure and from comparing the Sm(1)–Sm(2) and O(1)–O(2) distances in the cis and trans isomers. These distances are 7.20 and 3.05 Å, respectively, in the cis isomer, and 7.73 and 3.61 Å, respectively, in the trans isomer. The longer distances are consistent with the trans geometry. Disorder problems have also been observed in efforts to refine the structure of *trans*-[(C₅Me₅)₂ZrI]₂(μ-OCH=CHO).[13] One can easily rationalize disorder problems in trans enediolate ligands by realizing that when the two M–O bonds are colinear, rotation of the bridging group can occur without change in the coordinates of other atoms. The shapes of the thermal ellipsoids of C(1) and C(2) are consistent with the presence of this kind of rotational disorder.

Results

NMR Studies. [(C₅Me₅)₂SmH]₂ (I) displays high reactivity with a variety of substrates[23] and CO is no exception. Orange solutions of I in benzene or toluene reacted rapidly and cleanly with carbon monoxide at 1 atm or 90 psi to yield red brown solutions of a new complex II. The reaction of CO with I was initially followed by NMR spectroscopy by observing the ¹H chemical shift of the strong singlet due to the C₅Me₅ ligands. For I in benzene, this signal occurs at −0.80 ppm, shifted upfield and slightly broadened (half-width = 11 Hz) by the paramagnetic Sm(III) center ($\mu_{\text{eff}}^{297\text{ K}} = 1.4\ \mu_B$).[23] At 296 K, the new CO reaction product, II, also exhibited a single, but broader, signal (half-width = 16 Hz), in this case at −0.7 ppm. As described in the experimental section, the spectrum of II in toluene-d_8 underwent dramatic changes as the temperature was lowered. Solutions of II were observed to be stable for weeks at room temperature under nitrogen and did not react further with CO (90 psi, 5 days). No reaction was observed under 1 atm of hydrogen for 1 h.

The addition of coordinating ligands to NMR samples of II caused the C₅Me₅ signal to shift and sharpen. Triphenylphosphine oxide (TPPO) initially formed an adduct with a ¹H NMR C₅Me₅ signal at 1.68 ppm, IIIa. As described below, this compound subsequently was isolated and crystallographically identified as *cis*-{(C₅Me₅)₂[(C₆H₅)₃PO]Sm}₂(μ-OCH=CHO). On standing, dilute solutions of IIIa transformed quantitatively to IIIb, whose NMR signal appeared at 1.89 ppm. IIIb was also isolated and crystallographically characterized as *trans*-{(C₅Me₅)₂-[(C₆H₅)₃PO]Sm}₂(μ-OCH=CHO). When THF-d_8 was added to solutions of II, the C₅Me₅ signal also sharpened and shifted,

in this case to 1.76 ppm (IVa). On standing for hours to days, depending on concentration, a shoulder appeared on the downfield side, the shoulder grew at the expense of the 1.76 peak, and ultimately a new compound with a signal at 1.77 ppm, IVb, was formed. Surprisingly, this process occurred most rapidly in dilute solutions (see below). Addition of excess TPPO to freshly prepared solutions of IV generated a signal for IIIa at 1.68 ppm. Similarly, TPPO addition to solutions of IVb generated IIIb, with a signal at 1.89 ppm. This suggested that IVa is the THF adduct of the cis enediolate complex, i.e., *cis*-{(C₅Me₅)₂(THF)Sm}₂(μ-OCH=CHO), and IVb is the THF adduct of the trans isomer.

Product Isolation and Crystallization. In contrast to the tacky or glassy solids isolated from solutions of II, solutions of the TPPO adducts IIIa and IIIb formed crystalline solids which were more readily and completely characterizable. When TPPO was added to a solution of II in benzene, IIIa crystallized in large single platelike crystals. These crystals deteriorated over a period of hours even when loaded into an X-ray capillary tube directly from the mother liquor. However, pulverizing the crystals and drying them in vacuo gave a powder characterized as {(C₅Me₅)₂-[(C₆H₅)₃PO]Sm}₂(μ-OCH=CHO) by complete elemental analysis and by NMR spectroscopy (C₅Me₅ resonance at 1.68 ppm). Approximately 5% of IIIb, with a signal at 1.89 ppm, was also observed. The yield of crystalline IIIa formed by addition of TPPO to a benzene solution of II was moderate (37%) and rotary evaporation of the mother liquor gave a residue which contained additional IIIa as well as its isomer IIIb. Crystallization of IIIa from benzene and its conversion to IIIb in solution were evidently competitive processes.

When TPPO was added to a solution of II in *toluene*, crystallization did not occur. However, if the toluene was removed and benzene was added, IIIa formed as a microcrystalline solid. More stable crystals of IIIa were obtained by recrystallizing dry powdered IIIa from toluene under hexane diffusion overnight. This gave a mixture of polyhedra and tiny needles whose NMR spectrum revealed 33% IIIa (1.68 ppm) and 67% IIIb (1.89 ppm). On rinsing a sample of the crystals with hexane, the needles were unaffected, but the polyhedra became cloudy (presumably due to desolvation). Fully solvated polyhedra taken from the mother liquor of another crystallization were shown by X-ray diffraction to be *cis*-{(C₅Me₅)₂[(C₆H₅)₃PO]Sm}₂(μ-OCH=CHO) with three toluene molecules of crystallization per bimetallic unit. Recrystallization of the IIIa–IIIb mixture over a several-day period gave only large needles which were identified by NMR (1.89 ppm) and X-ray diffraction to be *trans*-{(C₅Me₅)₂[(C₆H₅)₃PO]Sm}₂-(μ-OCH=CHO) (IIIb), which crystallizes without lattice solvent.

These structural–spectral correlations yield the following interpretation of the observed chemistry. The cis isomer apparently requires solvent of crystallization in its structure. With benzene as the solvent, needles are formed which desolvate readily. With toluene, polyhedra are formed which are more stable with respect to desolvation but which will lose solvent upon washing with hexane. The cis isomer IIIa isomerizes to the trans isomer IIIb. Solvent of crystallization is not required in the structure of the trans isomer.

The IR spectra of IIIa and IIIb are also consistent with the above assignments and contain bands primarily interpretable in terms of coordinated C₅Me₅ and TPPO. In addition, a medium-intensity band occurs at 1600 cm^{-1} in IIIa which is absent in IIIb. This is consistent with a C=C stretch in a OCH=CHO group, which would be more intense in the infrared spectrum for a cis geometry as in IIIa than a trans geometry as in IIIb. By comparison, the infrared spectrum of II yields very little conclusive structural information. The base line rises to medium intensity from 1660 to 900 cm^{-1} and is capped with numerous distinct peaks from 1590 to 980 cm^{-1}.

Finally, it should be clarified that the addition of TPPO to solutions of II in arenes does not simply produce a mixture of IIIa and IIIb from which IIIa is selectively crystallized (in benzene). The NMR experiments demonstrates that IIIa is, in fact, the first formed adduct and subsequently isomerizes to IIIb. Since isomerization starts to occur as soon as IIIa is in solution, no solution
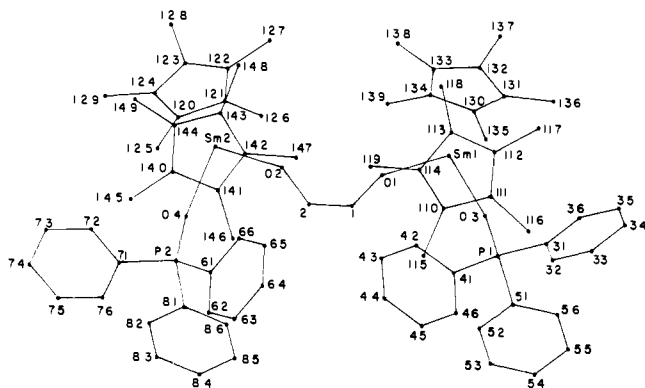
Reaction of the Samarium–H Bond in [(C₅Me₅)₂SmH]₂

J. Am. Chem. Soc., Vol. 107, No. 6, 1985 1675

Figure 1. Complete structure and numbering for *cis*-{(C₅Me₅)₂-[(C₆H₅)₃PO]Sm}₂(μ-OCH=CHO) (IIIa). Carbon atoms are labeled with their numbers only.

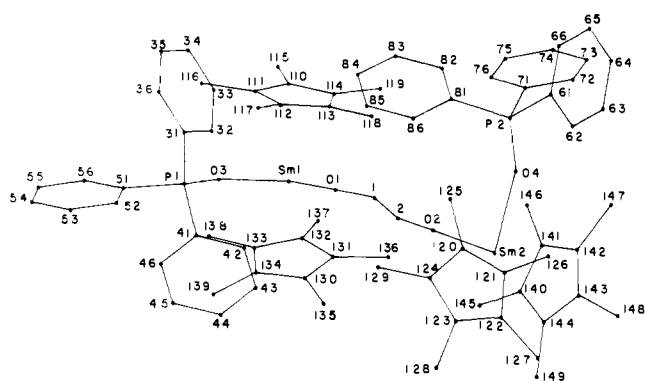**Figure 2.** Complete structure and numbering for *trans*-{(C₅Me₅)₂-[(C₆H₅)₃PO]Sm}₂(μ-OCH=CHO) (IIIb). Carbon atoms are labeled with their numbers only.

Figure 3. ORTEP drawing of *cis*-{(C₅Me₅)₂[(C₆H₅)₃PO]Sm}₂(μ-OCH=CHO) (IIIa), with phenyl groups deleted. Carbon atoms are labeled with their numbers only.

Figure 4. Comparison of the core atoms of *cis*- and *trans*-{(C₅Me₅)₂-[(C₆H₅)₃PO]Sm}₂(μ-OCH=CHO). The trans structure (bottom diagram) shows the large thermal ellipsoids for the bridge carbon atoms which would not refine to reasonable positions because of disorder.

of IIIa completely free of traces of IIIb has yet been observed. However, IIIa can be selectively isolated from benzene solutions that contain increasing amounts of IIIb by crystallization.

***cis*- to *trans*-{(C₅Me₅)₂[(C₆H₅)₃PO]Sm}₂(μ-OCH=CHO) Isomerization.** The isomerization of IIIa and IIIb was observed in benzene-*d₆* or toluene-*d₈* NMR solutions in which previously isolated IIIa powder had been dissolved. IIIa is only sparingly soluble in benzene-*d₆* and such dilute solutions isomerize over a period of several hours. IIIa is somewhat more soluble in toluene-*d₈* and these more concentrated solutions require days to isomerize. Isomerization also occurs in solutions of IIIa generated by adding excess triphenylphosphine oxide directly to NMR solutions of II. The slowest isomerization rates are observed for the most concentrated solutions of IIIa obtainable by reacting saturated solutions of I with CO in toluene-*d₈* and adding excess TPPO (benzene-*d₆* cannot be used because crystals form). These solutions require many days to isomerize. The effect of excess TPPO on the isomerization of IIIa was studied by dissolving IIIa in a C₆D₆ solution, which already contained dissolved TPPO. Isomerization proceeded in hours. Dilution of a sample of the latter solution with more of the TPPO/benzene solution hastened the isomerization. Hence, the isomerization is qualitatively more rapid as the initial concentration of dimer is reduced, regardless of the presence or absence of excess TPPO. Similar results were noted for the THF adducts, IVa and IVb.

Structures of IIIa and IIIb. The complete structures of *cis*- and *trans*-{(C₅Me₅)₂[(C₆H₅)₃PO]Sm}₂(μ-OCH=CHO) are shown in line and dot drawings in Figures 1 and 2, respectively. An ORTEP drawing of the cis isomer in which the phenyl groups are left out for clarity is shown in Figure 3. In both IIIa and IIIb, two crystallographically independent (C₅Me₅)₂Sm[OP(C₆H₅)₃] units are bridged by an enediolate ligand, —OCH=CHO—. The two C₅Me₅ ring centroids, the OPPh₃ oxygen atom, and the oxygen atom of the enediolate ligand which surround each samarium atom roughly comprise a distorted tetrahedron around the metal center.
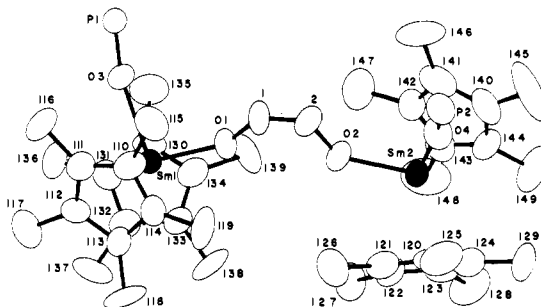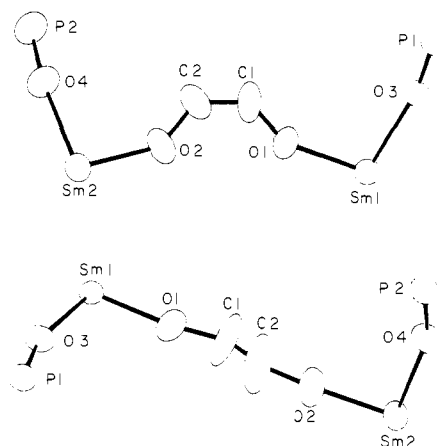
Positional parameters for IIIa and IIIb are given in Tables III and IV and bond lengths and angles are given in Tables V and VI.

The coordination geometry around each samarium atom is typical of bent metallocene molecules with two additional ligands,[32] and the structural parameters are similar to those in other (C₅Me₅)₂LnXY molecules. The ring centroid–metal–ring centroid angles, 132.6° (Sm(1), IIIa), 133.2° (Sm(2), IIIa), 132.6° (Sm(1), IIIb), and 131.4° (Sm(2), IIIb), are within the 131–138° range normally found for lanthanide complexes of this class.[33,34] The average Sm–C(ring) distances for IIIa, 2.77 Å, and IIIb, 2.76 Å, are on the higher end of the range of average values observed for other (C₅Me₅)₂SmXY systems: (C₅Me₅)₂SmCl(THF) (V)[33] 2.72 Å, (C₅Me₅)₂SmI(THF) (VI)[33] 2.72 Å, (C₅Me₅)₂Sm(C₆H₅)(THF) (VII)[35] 2.735 Å, [(C₅Me₅)₂Sm]₂(μ-O)[36] 2.74 Å, and [(C₅Me₅)₂SmH]₂[23] 2.755 Å. The average Sm–O(TPPO) distances in IIIa, 2.39 Å, and IIIb, 2.37 Å, are significantly shorter than the average Sm–O(THF) distances in V, 2.46 Å, VI, 2.45 Å, and VII, 2.51 Å. Complexes IIIa and IIIb are to our knowledge the first crystallographically characterized examples of triphenylphosphine oxide adducts of organolanthanide complexes.[37] The Sm–O(TPPO) distances in IIIa and IIIb are roughly comparable to the average U–O(TPPO) distances in (C₅H₅)UCl₃[OP(C₆-

(32) Lauher, J. W.; Hoffmann, R. *J. Am. Chem. Soc.* **1976**, *98*, 1729–1742.

(33) Evans, W. J.; Grate, J. W.; Levan, K. W.; Doedens, R. J.; Hunter, W. E.; Zhang, H.; Atwood, J. L., manuscript in preparation.

(34) This is also within the 128–139° range found for (C₅Me₅)₂MXY complexes where M is U or Th: Bruno, J. W.; Marks, T. J.; Day, V. W. *J. Organomet. Chem.* **1983**, *250*, 237–246.

(35) Evans, W. J.; Bloom, I.; Hunter, W. E.; Atwood, J. L. *Organometallics* **1985**, *4*, 112–119.

(36) Evans, W. J.; Grate, J. W.; Bloom, I.; Hunter, W. E.; Atwood, J. L. *J. Am. Chem. Soc.* **1985**, *107*, 405–409.

(37) Cf.: Forsberg, J. H.; Moeller, T. In "Gmelin Handbook of Inorganic Chemistry"; 8th ed.; Moeller, T.; Krüerke, U.; Schleitzer-Rust, E., Eds.; Springer-Verlag: New York, 1983; Sc, Y, La–Lu, Vol. D6, pp 137–302.

Table III. Atomic Positional Parameters for
cis-{(C₅Me₅)₂[(C₆H₅)₃PO]Sm}₂(μ-OCH=CHO)

atom	x	y	z
Sm(1)	0.16424 (5)	0.25878 (5)	0.48763 (6)
Sm(2)	0.52083 (5)	0.31293 (5)	0.72981 (6)
P(1)	0.0317 (2)	0.2884 (2)	0.6927 (3)
P(2)	0.5165 (3)	0.1474 (3)	0.8724 (3)
O(1)	0.2531 (6)	0.2604 (6)	0.5933 (8)
O(2)	0.4080 (6)	0.2780 (6)	0.6838 (8)
O(3)	0.0744 (5)	0.2739 (6)	0.6038 (7)
O(4)	0.5260 (6)	0.2155 (6)	0.8253 (8)
C(1)	0.2813 (19)	0.2401 (10)	0.6722 (14)
C(2)	0.3476 (10)	0.2479 (10)	0.7143 (13)
C(110)	0.1439 (11)	0.1001 (9)	0.4692 (14)
C(111)	0.0794 (10)	0.1214 (8)	0.4178 (14)
C(112)	0.0993 (10)	0.1441 (9)	0.3345 (12)
C(113)	0.1755 (9)	0.1366 (9)	0.3246 (13)
C(114)	0.2022 (10)	0.1106 (9)	0.4132 (13)
C(115)	0.1474 (11)	0.0693 (10)	0.5638 (13)
C(116)	0.0021 (10)	0.1116 (11)	0.4511 (15)
C(117)	0.0459 (11)	0.1572 (11)	0.2538 (14)
C(118)	0.2168 (11)	0.1413 (11)	0.2356 (15)
C(119)	0.2786 (10)	0.0916 (11)	0.4340 (16)
C(120)	0.5951 (12)	0.2034 (12)	0.6001 (13)
C(121)	0.5337 (11)	0.2252 (13)	0.5423 (15)
C(122)	0.5467 (11)	0.3019 (15)	0.5343 (15)
C(123)	0.6142 (11)	0.3323 (11)	0.5890 (14)
C(124)	0.6441 (11)	0.2735 (12)	0.6303 (14)
C(125)	0.6095 (12)	0.1248 (11)	0.6172 (16)
C(126)	0.4712 (12)	0.1699 (13)	0.4912 (15)
C(127)	0.4988 (11)	0.3476 (15)	0.4756 (15)
C(128)	0.6569 (11)	0.4080 (11)	0.5837 (17)
C(129)	0.7165 (10)	0.2781 (13)	0.6860 (16)
C(130)	0.1496 (11)	0.4165 (10)	0.5090 (13)
C(131)	0.1135 (10)	0.3833 (9)	0.4165 (13)
C(132)	0.1676 (11)	0.3553 (9)	0.3511 (14)
C(133)	0.2351 (10)	0.3678 (10)	0.4081 (14)
C(134)	0.2242 (10)	0.4069 (10)	0.5047 (15)
C(135)	0.1147 (11)	0.4625 (11)	0.6004 (14)
C(136)	0.0351 (9)	0.3888 (11)	0.3889 (14)
C(137)	0.1543 (12)	0.3297 (11)	0.2392 (12)
C(138)	0.3046 (10)	0.3484 (12)	0.3662 (16)
C(139)	0.2839 (11)	0.4365 (10)	0.5894 (13)
C(140)	0.5688 (14)	0.4072 (12)	0.9087 (15)
C(141)	0.4905 (14)	0.4016 (11)	0.9050 (14)
C(142)	0.4690 (10)	0.4444 (10)	0.8359 (14)
C(143)	0.5297 (13)	0.4734 (10)	0.7952 (14)
C(144)	0.5919 (10)	0.4492 (12)	0.8421 (17)
C(145)	0.6175 (15)	0.3730 (12)	0.9798 (18)
C(146)	0.4398 (13)	0.3686 (12)	0.9704 (16)
C(147)	0.3895 (11)	0.4566 (12)	0.8095 (17)
C(148)	0.5295 (14)	0.5305 (11)	0.7230 (16)
C(149)	0.6678 (12)	0.4767 (14)	0.8451 (21)
C(901)	0.1183 (21)	0.5652 (22)	0.9172 (28)
C(902)	0.1477 (18)	0.6319 (20)	1.0190 (24)
C(903)	0.1324 (15)	0.7102 (17)	1.0516 (20)
C(904)	0.0798 (19)	0.7770 (22)	0.9993 (28)
C(905)	0.0680 (19)	0.7038 (24)	0.9206 (28)
C(906)	0.0765 (22)	0.6296 (27)	0.8815 (29)
C(911)	0.2209 (14)	0.0887 (16)	0.8383 (19)
C(912)	0.2001 (16)	0.1540 (16)	0.9082 (22)
C(913)	0.1430 (16)	0.1282 (18)	0.9672 (21)
C(914)	0.1222 (17)	0.0511 (21)	0.9409 (23)
C(915)	0.1429 (21)	0.0094 (21)	0.8784 (29)
C(916)	0.1892 (21)	0.0055 (22)	0.8241 (27)
C(921)	0.2644 (23)	0.7665 (22)	0.6026 (27)
C(922)	0.3050 (17)	0.7268 (18)	0.6509 (23)
C(923)	0.3198 (28)	0.6836 (26)	0.7565 (34)
C(924)	0.2460 (34)	0.7107 (30)	0.7641 (39)
C(925)	0.1950 (22)	0.7460 (23)	0.7185 (30)
C(926)	0.1941 (24)	0.7923 (23)	0.6077 (31)

H₅)₃]₂·THF,[38] 2.31 Å, when the 0.034[39]–0.079[40] Å difference in metallic radii is considered.

(38) Bombieri, G.; de Paoli, G.; Del Pra, A.; Bagnall, K. W. *Inorg. Nucl. Chem. Lett.* **1978**, *14*, 359.

(39) Cotton, F. A.; Wilkinson, G. "Advanced Inorganic Chemistry", 4th ed.; Wiley: New York, 1980.

Table IV. Atomic Positional Parameters for
trans-{(C₅Me₅)₂[(C₆H₅)₃PO]Sm}₂(μ-OCH=CHO)

atom	x	y	z
Sm(1)	0.33894 (4)	0.75621 (3)	0.42034 (2)
Sm(2)	0.18528 (4)	0.68092 (3)	0.64582 (2)
P(1)	0.2758 (2)	0.5904 (2)	0.3431 (1)
P(2)	0.0075 (2)	0.8187 (2)	0.5907 (1)
O(1)	0.3026 (6)	0.7290 (5)	0.4696 (3)
O(2)	0.2242 (6)	0.6914 (5)	0.5791 (3)
O(3)	0.3269 (5)	0.6604 (4)	0.3657 (2)
O(4)	0.0615 (5)	0.7702 (4)	0.6226 (3)
C(1)	0.2675 (13)	0.7262 (14)	0.5092 (7)
C(2)	0.2632 (11)	0.7071 (14)	0.5402 (5)
C(110)	0.2487 (8)	0.8454 (6)	0.3706 (4)
C(111)	0.3186 (9)	0.8468 (6)	0.3430 (4)
C(112)	0.3942 (9)	0.8907 (7)	0.3674 (5)
C(113)	0.3701 (10)	0.9147 (7)	0.4106 (5)
C(114)	0.2815 (10)	0.8874 (6)	0.4120 (4)
C(115)	0.1537 (9)	0.8087 (8)	0.3578 (6)
C(116)	0.3130 (12)	0.8100 (8)	0.2943 (4)
C(117)	0.4776 (11)	0.9176 (9)	0.3455 (6)
C(118)	0.4250 (13)	0.9682 (8)	0.4475 (6)
C(119)	0.2251 (12)	0.9024 (9)	0.4512 (5)
C(120)	0.0461 (9)	0.5741 (7)	0.6261 (6)
C(121)	0.0609 (9)	0.5775 (7)	0.6743 (5)
C(122)	0.1477 (9)	0.5475 (8)	0.6925 (5)
C(123)	0.1889 (10)	0.5253 (8)	0.6546 (6)
C(124)	0.1248 (11)	0.5410 (7)	0.6117 (5)
C(125)	0.0448 (12)	0.5959 (10)	0.5922 (7)
C(126)	0.0102 (12)	0.6016 (10)	0.7052 (7)
C(127)	0.1819 (13)	0.5275 (11)	0.7455 (6)
C(128)	0.2859 (13)	0.4835 (11)	0.6610 (10)
C(129)	0.1329 (16)	0.5208 (11)	0.5616 (6)
C(130)	0.5163 (7)	0.6758 (6)	0.4831 (4)
C(131)	0.5402 (7)	0.7537 (6)	0.4917 (4)
C(132)	0.5769 (8)	0.7824 (7)	0.4527 (4)
C(133)	0.5732 (7)	0.7217 (7)	0.4192 (4)
C(134)	0.5363 (7)	0.6565 (6)	0.4380 (4)
C(135)	0.4773 (8)	0.6211 (7)	0.5166 (4)
C(136)	0.5349 (10)	0.7970 (8)	0.5378 (4)
C(137)	0.6272 (9)	0.8584 (8)	0.4527 (6)
C(138)	0.6106 (10)	0.7258 (8)	0.3728 (5)
C(139)	0.5301 (9)	0.5747 (7)	0.4169 (4)
C(140)	0.3577 (8)	0.7410 (9)	0.6789 (5)
C(141)	0.2975 (9)	0.8050 (8)	0.6733 (5)
C(142)	0.2444 (9)	0.7960 (10)	0.7091 (6)
C(143)	0.2722 (11)	0.7325 (11)	0.7358 (5)
C(144)	0.3408 (9)	0.6960 (9)	0.7182 (5)
C(145)	0.4330 (10)	0.7265 (13)	0.6492 (6)
C(146)	0.3014 (16)	0.8678 (11)	0.6365 (6)
C(147)	0.1674 (13)	0.8587 (14)	0.7156 (8)
C(148)	0.2400 (15)	0.7086 (15)	0.7829 (6)
C(149)	0.4045 (12)	0.6289 (12)	0.7414 (6)
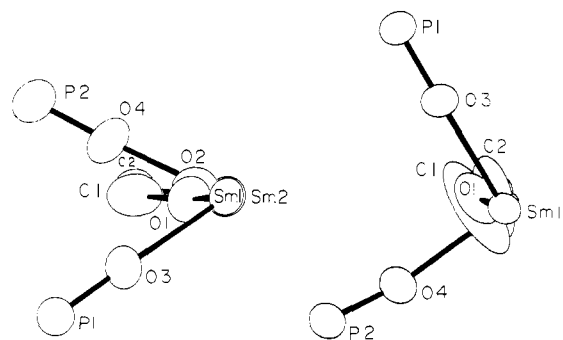
Figure 5. View of the POSmOCCOSmOP unit of *cis*- and *trans*-{(C₅Me₅)₂[(C₆H₅)₃Sm]₂(μ-OCH=CHO) viewed down the Sm–Sm vector. The cis structure is on the left.

A discussion of distances and angles in the enediolate bridge will be limited to the cis isomer IIIa, since in the trans isomer disorder exists in the positions of the enediolate carbon atoms.

(40) Shannon, R. D. *Acta Crystallogr., Sect. A* **1976**, *A32*, 751–767.

Reaction of the Samarium-H Bond in [(C₅Me₅)₂SmH]₂

J. Am. Chem. Soc., Vol. 107, No. 6, 1985 1677

Table V. Interatomic Distances (Å) in *cis*- and *trans*-{(C₅Me₅)₂[(C₆H₅)₃PO]Sm}₂(μ-OCH=CHO)

	cis	trans
Sm(1)-O(1)	2.147 (10)	2.122 (8)
Sm(2)-O(2)	2.179 (10)	2.107 (7)
Sm(1)-O(3)	2.392 (10)	2.355 (7)
Sm(2)-O(4)	2.393 (10)	2.391 (7)
Sm(1)-C(110)	2.759 (15)	2.757 (10)
Sm(1)-C(111)	2.776 (16)	2.764 (11)
Sm(1)-C(112)	2.773 (16)	2.802 (11)
Sm(1)-C(113)	2.807 (15)	2.784 (11)
Sm(1)-C(114)	2.747 (15)	2.762 (11)
Sm(1)-C(11X av)	2.77	2.77
Sm(1)-C(130)	2.764 (17)	2.732 (10)
Sm(1)-C(131)	2.785 (15)	2.731 (10)
Sm(1)-C(132)	2.817 (17)	2.782 (11)
Sm(1)-C(133)	2.739 (15)	2.777 (11)
Sm(1)-C(134)	2.741 (16)	2.748 (10)
Sm(1)-C(13X av)	2.77	2.75
Sm(2)-C(120)	2.837 (19)	2.744 (12)
Sm(2)-C(121)	2.774 (18)	2.794 (12)
Sm(2)-C(122)	2.771 (19)	2.790 (13)
Sm(2)-C(123)	2.771 (17)	2.723 (13)
Sm(2)-C(124)	2.807 (19)	2.714 (13)
Sm(2)-C(12X av)	2.79	2.75
Sm(2)-C(140)	2.755 (17)	2.741 (11)
Sm(2)-C(141)	2.718 (19)	2.744 (13)
Sm(2)-C(142)	2.732 (16)	2.738 (13)
Sm(2)-C(143)	2.774 (17)	2.811 (13)
Sm(2)-C(144)	2.788 (17)	2.802 (13)
Sm(2)-C(14X av)	2.75	2.77
P(1)-O(3)	1.501 (10)	1.514 (7)
P(2)-O(4)	1.496 (11)	1.495 (8)
O(1)-C(1)	1.319 (19)	1.334 (15)
O(2)-C(2)	1.352 (18)	1.374 (17)
C(1)-C(2)	1.324 (22)	0.964 (18)
C(110)-C(114)	1.406 (22)	1.404 (16)
C(110)-C(111)	1.472 (23)	1.408 (16)
C(110)-C(115)	1.532 (23)	1.516 (18)
C(111)-C(112)	1.375 (21)	1.421 (17)
C(111)-C(116)	1.556 (23)	1.528 (16)
C(112)-C(113)	1.449 (22)	1.416 (18)
C(112)-C(117)	1.522 (23)	1.549 (18)
C(113)-C(114)	1.478 (22)	1.392 (18)
C(113)-C(118)	1.518 (23)	1.525 (18)
C(114)-C(119)	1.508 (23)	1.539 (18)
C(120)-C(121)	1.477 (26)	1.363 (18)
C(120)-C(124)	1.466 (24)	1.420 (18)
C(120)-C(125)	1.492 (25)	1.547 (18)
C(121)-C(122)	1.391 (26)	1.387 (17)
C(121)-C(126)	1.515 (25)	1.548 (17)
C(122)-C(123)	1.446 (25)	1.395 (19)
C(122)-C(127)	1.547 (27)	1.552 (19)
C(123)-C(124)	1.415 (24)	1.432 (20)
C(123)-C(128)	1.535 (24)	1.579 (20)
C(124)-C(129)	1.507 (25)	1.508 (20)
C(130)-C(131)	1.411 (21)	1.412 (15)
C(130)-C(134)	1.416 (23)	1.421 (15)
C(130)-C(135)	1.559 (24)	1.538 (15)
C(131)-C(132)	1.441 (23)	1.421 (16)
C(131)-C(136)	1.504 (23)	1.539 (16)
C(132)-C(133)	1.429 (22)	1.424 (16)
C(132)-C(137)	1.532 (23)	1.516 (17)
C(133)-C(134)	1.410 (22)	1.409 (15)
C(133)-C(138)	1.484 (23)	1.535 (16)
C(134)-C(139)	1.556 (23)	1.545 (15)
C(140)-C(141)	1.457 (28)	1.413 (18)
C(140)-C(144)	1.383 (26)	1.434 (19)
C(140)-C(145)	1.544 (27)	1.537 (18)
C(141)-C(142)	1.401 (24)	1.410 (20)
C(141)-C(146)	1.532 (27)	1.530 (22)
C(142)-C(143)	1.418 (25)	1.365 (22)
C(142)-C(147)	1.545 (25)	1.607 (23)
C(143)-C(144)	1.428 (24)	1.365 (20)
C(143)-C(148)	1.571 (26)	1.570 (21)
C(144)-C(149)	1.468 (25)	1.567 (22)

Table VI. Bond Angles (deg) for *cis*- and *trans*-{(C₅Me₅)₂[(C₆H₅)₃PO]Sm}₂(μ-OCH=CHO)

	cis	trans
O(1)-Sm(1)-O(3)	95.7 (4)	94.7 (3)
O(2)-Sm(2)-O(4)	90.9 (4)	90.6 (3)
C(1)-O(1)-Sm(1)	150.7 (11)	161.9 (14)
C(2)-O(2)-Sm(2)	142.1 (11)	168.8 (10)
P(1)-O(3)-Sm(1)	167.6 (6)	163.0 (5)
P(2)-O(4)-Sm(2)	168.8 (7)	158.7 (5)
O(1)-C(1)-C(2)	132.5 (18)	154.5 (20)
C(1)-C(2)-O(2)	128.4 (18)	158.2 (18)
C(114)-C(110)-C(111)	107.1 (15)	107.3 (12)
C(114)-C(110)-C(115)	125.8 (18)	125.5 (12)
C(111)-C(110)-C(115)	127.0 (18)	127.2 (12)
C(112)C(111)-C(110)	108.5 (16)	108.4 (11)
C(112)-C(111)-C(116)	127.8 (18)	125.6 (12)
C(110)-C(111)-C(116)	123.5 (17)	126.0 (12)
C(111)-C(112)-C(113)	110.4 (16)	107.0 (11)
C(111)-C(112)-C(117)	123.7 (18)	124.5 (13)
C(113)-C(112)-C(117)	124.6 (17)	127.7 (13)
C(112)-C(113)-C(114)	105.0 (15)	108.1 (11)
C(112)-C(113)-C(118)	127.6 (17)	127.2 (14)
C(114)-C(113)-C(118)	126.7 (16)	124.4 (14)
C(110)-C(114)-C(113)	108.9 (15)	109.2 (18)
C(110)-C(114)-C(119)	126.2 (18)	124.2 (13)
C(113)-C(114)-C(119)	124.7 (18)	126.5 (13)
C(124)-C(120)-C(121)	106.1 (17)	109.2 (11)
C(124)-C(120)-C(125)	125.6 (20)	124.7 (16)
C(121)-C(120)-C(125)	128.0 (20)	125.9 (15)
C(122)-C(121)-C(120)	108.8 (18)	109.2 (12)
C(122)-C(121)-C(126)	125.9 (23)	123.8 (14)
C(120)-C(121)-C(126)	125.0 (21)	126.7 (13)
C(121)-C(122)-C(123)	108.4 (19)	108.1 (13)
C(121)-C(122)-C(127)	126.7 (22)	124.2 (14)
C(123)-C(122)-C(127)	125.0 (22)	126.6 (14)
C(124)-C(123)-C(122)	109.3 (17)	108.0 (12)
C(124)-C(123)-C(128)	123.1 (20)	128.5 (17)
C(122)-C(123)-C(128)	126.0 (21)	123.3 (17)
C(123)-C(124)-C(20)	107.4 (18)	105.5 (11)
C(123)—C(124)-C(129)	127.0 (19)	128.5 (16)
C(120)-C(124)-C(129)	125.3 (19)	125.8 (16)
C(131)-C(130)-C(134)	109.6 (16)	107.5 (10)
C(131)-C(130)-C(135)	125.9 (18)	126.5 (10)
C(134)-C(130)-C(135)	124.4 (18)	126.0 (11)
C(130)-C(131)-C(132)	107.0 (16)	108.6 (10)
C(130)-C(131)-C(136)	125.4 (18)	124.8 (11)
C(132)-C(131)-C(136)	126.9 (17)	126.4 (11)
C(133)-C(132)-C(131)	107.2 (16)	107.4 (10)
C(133)-C(132)-C(137)	127.7 (18)	127.3 (11)
C(131)-C(132)-C(137)	124.5 (18)	124.3 (12)
C(134)-C(133)-C(132)	108.8 (16)	108.0 (10)
C(134)-C(133)-C(138)	127.5 (18)	126.6 (11)
C(132)-C(133)-C(138)	123.5 (18)	125.3 (11)
C(133)-C(134)-C(130)	107.4 (16)	108.5 (10)
C(133)-C(134)-C(139)	126.0 (18)	126.3 (10)
C(130)-C(134)-C(139)	126.6 (18)	124.7 (10)
C(144)-C(140)-C(141)	110.0 (19)	109.0 (12)
C(144)-C(140)-C(145)	126.0 (26)	126.5 (15)
C(141)-C(140)-C(145)	124.0 (25)	124.4 (16)
C(142)-C(141)-C(140)	104.8 (19)	132.9 (16)
C(142)-C(141)-C(146)	124.6 (24)	104.3 (13)
C(140)-C(141)-C(146)	130.0 (22)	122.7 (6)
C(141)-C(142)-C(143)	110.5 (18)	110.6 (13)
C(141)-C(142)-C(147)	123.3 (22)	120.3 (19)
C(143)-C(142)-C(147)	126.2 (20)	129.0 (18)
C(142)-C(143)-C(144)	106.9 (17)	109.5 (13)
C(142)-C(143)-C(148)	126.6 (21)	126.4 (17)
C(144)-C(143)-C(148)	126.1 (22)	123.8 (18)
C(140)-C(144)-C(143)	107.8 (18)	106.5 (14)
C(140)-C(144)-C(149)	120.6 (25)	124.5 (14)
C(143)-C(144)-C(149)	129.8 (24)	127.8 (15)

This can be clearly seen in Figures 4 and 5, which compare the (POSₘ)₂(μ-OCH=CHO) units in the two isomers with a side view

and a view down the Sm–Sm vector, respectively. As detailed in the experimental section, in the trans configuration the carbon atoms can reside in a variety of positions which are still consistent with the bonding requirements of the remainder of the molecule. This is not true for the cis isomer, and well-defined carbon positions are observed.

1678 *J. Am. Chem. Soc., Vol. 107, No. 6, 1985*
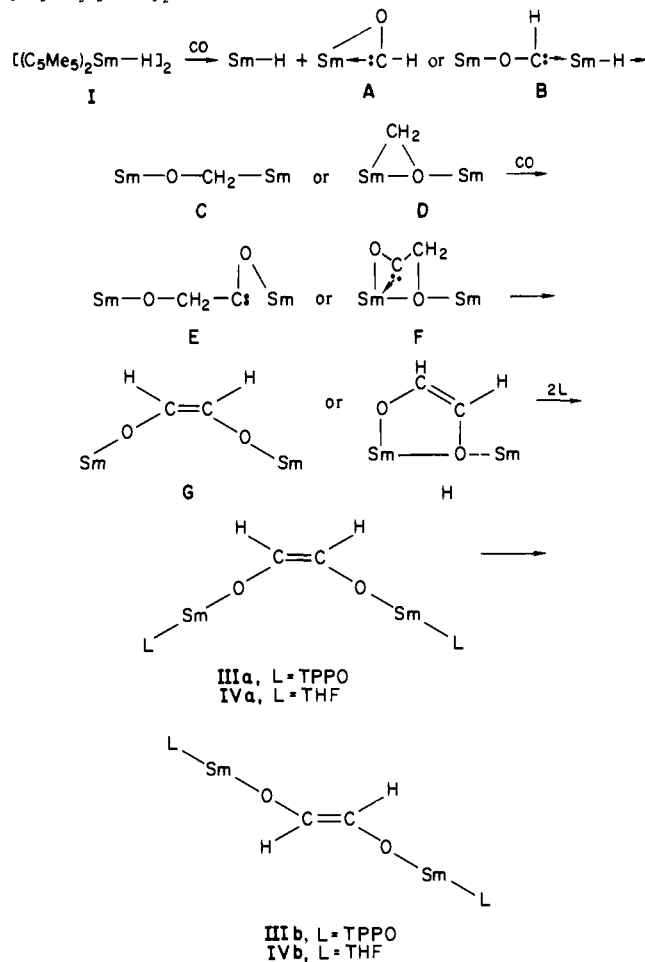
Evans, Grate, and Doedens

As shown in Figure 5, the SmOCH=CHOSm unit in IIIa is nearly planar. The Sm—O distances of 2.147 (10) and 2.179 (10) Å are longer than that found in [(C₅Me₅)₂Sm](μ-O),[36] 2.094 (1) Å, which had an unusually short metal oxygen interaction and a 180° Sm–O–Sm angle. The Sm–O distances in IIIa are comparable to the Lu—O—C distance in [(C₅H₅)₂Lu]₂(OC)₄(CMe₃)₂[18] (see eq 2), 2.091 (8) Å, when the difference in radii of Sm(III) and Lu(III), 0.116[39]–0.102[40] Å, is considered. The C=C bond length of 1.324 (22) Å in IIIa is reasonable for a C=C double bond[41] and is similar to that found in the methyl-substituted cis enediolate in [(C₅Me₅)₂Th]₂[μ-OC(CH₃)=C(CH₃)O]₂ (VIII), 1.33 (2) Å.[42] The torsion angle about the C=C bond is 2.9°. The C—O bond distances in IIIa, 1.319 (19) and 1.352 (18) Å, are shorter than normally observed for alcoholic C—O[41] and shorter than the analogous C–O bond length in VIII, 1.37 (2) Å. Consistent with the relative shortness of the C—O bond, the O—C=C angles of 132.51 (179)° and 128.38 (175)° are larger than expected for a simple sp² carbon atom. In VIII, the analogous O—C=C angle is 122 (1)°. The largest O—C=C angle and the longest O—C bond in IIIa are at the same end of the enediolate bridge.

Discussion

The formation of the enediolate moiety in {(C₅Me₅)₂[(C₆H₅)₃PO]Sm}₂(μ-OCH=CHO) from the reaction of [(C₅Me₅)₂SmH]₂ with CO demonstrates that lanthanide hydrides are capable of both reducing CO and inducing C=C double-bond formation with this substrate. Given the complexity of the early transition-metal[11] and actinide[43] hydride reactions with CO, it is likely that full elucidation of the mechanistic aspects of this samarium-based CO reduction and homologation system will require detailed kinetic studies. However, some discussion on possible reaction pathways is appropriate at this point.

Scheme I shows several possible intermediates that may be present in this system. Note that only those species identified with a Roman numeral have been definitely characterized at this stage and that other possible intermediates exist. As shown in the scheme, the reaction of I with CO could proceed via monometallic η²-formyl complexes, e.g., A,[44] or via bimetallic oxycarbene complexes, e.g., B.[45,49] In either case, a Sm–O–CH₂–Sm unit as in C[51] or D[52] is a likely intermediate.[54] Either C or D could

(41) *Spec. Publ.—Chem. Soc.* **1965**, *No. 18*, M665. Cardin, D. J.; Cetinkaya, T. J.; Lappert, M. F. *Chem. Rev.* **1972**, *72*, 545–574. Allen, F. H.; Kirby, A. J. *J. Am. Chem. Soc.* **1984**, *106*, 6197–6200.

(42) Manriquez, J. M.; Fagan, P. J.; Marks, T. J.; Day, C. S.; Day, V. W. *J. Am. Chem. Soc.* **1978**, *100*, 7112.

(43) Katahira, D. A.; Moloy, K. G.; Marks, T. J. *Organometallics* **1982**, *1*, 1723–1726.

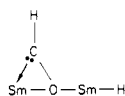(44) Cf. (C₅Me₅)₂Th[OC(CMe₃)₂H](OCH)[17] and (C₅H₅)₂LuOC(CMe₃).[18]

(45) Cf. (C₅H₅)₂(H)NbCHOZr(H)(C₅Me₅)₂.[46–48]

(46) Wolczanski, P. T.; Threlkel, R. S.; Bercaw, J. E. *J. Am. Chem. Soc.* **1979**, *101*, 218–220.

(47) Threlkel, R. S.; Bercaw, J. E. *J. Am. Chem. Soc.* **1981**, *103*, 2650–2659.

(48) Barger, P. T.; Bercaw, J. E. *Organometallics* **1984**, *3*, 278–284.

(49) Several other bimetallic structures with this formula are possible. An oxygen-bridged species, **B′**,

is conceivable on the basis of the zirconium structure [(C₅H₅)₂Zr]₂(H)(μ-H)(μ-OCHCH₃)[50] and related intermediates in that system.[11] Alternatively, the terminal hydride ligand in B and B′ could be bridging or the bimetallic complex could be held together solely by a hydride bridge, i.e., HCO–Sm–H–Sm.

(50) Erker, G.; Kropp, K.; Krüger, C.; Chiang, A.-P. *Chem. Ber.* **1982**, *115*, 2247–2460.

(51) Cf. the formation of [(C₅H₅)₂ZrCl]₂(μ-OCH₂)[15] and (C₅H₅)₂(CO)-Nb–CH₂O–Zr(H)(C₅Me₅)₂.[10,46]

(52) Cf. [(C₅H₅)₂Zr]₂(H)(μ-H)(μ-OCHCH₃),[50] [(C₅H₅)₂Zr(μ-CH₂O)]₃,[53] and related complexes.[11]

(53) Kropp, K.; Skibbe, V.; Erker, G.; Kruger, C. *J. Am. Chem. Soc.* **1983**, *105*, 3353–3354.

Scheme I. Possible Intermediates in the Formation of *cis*- and *trans*-{(C₅Me₅)₂[(C₆H₅)₃PO]Sm}₂(μ-OCH=CHO) from [(C₅Me₅)₂SmH]₂ and CO[a]

IIIa, L=TPPO
IVa, L=THF

IIIb, L=TPPO
IVb, L=THF

[a] Except in the first line the two C₅Me₅ groups per samarium have not been included in the formulas. L = TPPO or THF.

insert a second molecule of CO to generate a product such as E or F containing the two CO substrate units per samarium found in the final crystallographically characterized products.[55] Hydrogen migration would give an enediolate unit, e.g., G or H.[56,57] After TPPO addition, the *cis*-enediolate complex IIIa is isolated and this species subsequently rearranges to the trans isomer IIIb.[58]

Since the initially formed [(C₅Me₅)₂SmH]₂/CO reaction product, II, is spectroscopically complex (multiple IR absorptions; broad, temperature-dependent NMR signals) it is not evident which intermediate or intermediates form at this stage. However, it is clear that after adduct formation with TPPO or THF, a bridging enediolate ligand with cis geometry is present, i.e., IIIa. The exclusive initial formation of a cis enediolate in IIIa, a system that easily isomerizes to the trans form IIIb, suggests that the

(54) Direct coupling of two (C₅Me₅)₂SmOCH units to form (C₅Me₅)₂SmOCH=CHOSm(C₅Me₅)₂ is conceivable,[10,13] but it is unlikely since steric effects would not be expected to form the cis isomer exclusively. See also ref 43.

(55) Cf. ref 10, 11, 18, and 43.

(56) This has precedent in early transition-metal[11] and actinide systems.[43] For example, the hydrogen migration in the (C₅H₅)₂NbCH₂OZrH(C₅Me₅)₂ ⇌ (C₅H₅)₂HNb=CHOZrH(C₅Me₅)₂ tautomerization[47] is a metal-substituted analogue of this conversion in which the (C₅Me₅)₂Nb unit is acting like the carbene carbon atom in the (C₅Me₅)₂SmOC: unit.

(57) Spectroscopic, kinetic, and chemical studies on the (C₅Me₅)₂ThH-(OR)/CO system support a mechanism analogous to the A → C → E → G conversions.[43]

(58) Selectivity for *cis*-enediolate formation has precedent in the reaction of (C₅Me₅)₂ThH(Or) complexes with CO,[17,43] in the reaction of (C₅Me₅)₂ZrH₂ with (C₅Me₅)₂Zr(CO)₂ under H₂,[46] and in the [(C₅H₅)₂Zr]₂(H)(μ-H)(μ-OCHC₆H₅)/CO system.[11] However, the enediolate produced in the reaction of (C₅Me₅)₂ZrH₂ with CO is exclusively trans.[13]

enediolate formation and isomerization proceed by separate pathways. Common intermediates and facile reversible interconversion of intermediates seem unlikely. Since rotation about the C–C single bond in intermediate E would allow the formation of *both* cis and trans enediolate ligands, the alternative intermediate at this stage of the reaction, F, is an attractive candidate in the enediolate formation sequence. The multiple coordination of the OCCH₂O ligand in F might direct the hydrogen migration step to the cis geometry via a species such as H. Once a coordinating base such as TPPO or THF is added, reversible access to such cis-directing species may be prohibited.

The concentration-dependent isomerization of the cis enediolate to the trans enediolate, observed with both TPPO and THF adducts, is more difficult to explain. The isomerization of bridging enediolate ligands has not been previously observed. The closest related system known to isomerize is the cis enolate ligand of $(C_5Me_5)_2Zr^1(cis\text{-}OCH=CHR)$, formed initially by hydrogenation of a $C,O\text{-}\eta^2$-ketene ligand.[59] This compound isomerizes to the trans isomer at 80 °C.[59]

One simple mechanism for the room-temperature isomerization observed in our system would be to assume that the cis products, IIIa and IVa, are kinetic products which isomerize to the thermodynamic products IIIb and IVb, e.g., by rotation about the carbon single bond of an intermediate that has a structure like that of E. Formation of such trans-directing intermediates not accessible in the enediolate formation sequence may be possible in the presence of TPPO or THF. However, such a simplified process would not display the observed rate enhancement on

dilution. A more detailed kinetic analysis of this isomerization is necessary before the interesting concentration dependence of this conversion can be explained.

Conclusion

The ability of lanthanide hydride moieties to reduce and couple CO has been demonstrated in this study. This reaction system also has provided the first structural results on a product derived from the reaction of a lanthanide hydride with CO and the first refinable structural data on any enediolate unit derived from CO and a metal hydride. The fact that the cis enediolate unit, initially formed in this reaction, isomerizes to the trans isomer, a previously unobserved transformation in CO/metal hydride chemistry, raises interesting questions regarding the bonding and stability of the enediolate unit in general. Whether such transformations occur and are observable in other CO/metal hydride system or whether this isomerization is unique to lanthanide-based systems is a question deserving further study.

Registry No. I, 84751-30-4; IIIa, 94800-57-4; IIIa·3toluene, 94800-58-5; IIIb, 94842-40-7; IVa, 94800-59-6; IVb, 94842-41-8.

Supplementary Material Available: Tables of bond distances and angles for toluene molecules, atomic parameters for group atoms, thermal parameters, and observed and calculated structure factor amplitudes (74 pages). Ordering information is given on any current masthead page.

(59) Moore, E. J.; Straus, D. A.; Armantrout, J.; Santarsiero, B. D.; Grubbs, R. H.; Bercaw, J. A. *J. Am. Chem. Soc.* **1983**, *105*, 2068–2070.

Preparation and X-ray Structure Determination of [Li₆Br₄(Et₂O)₁₀]²⁺[Ag₃Li₂Ph₆]⁻₂: An Unusual Cation Composed of a Solvated "Salt Cluster"

Michael Y. Chiang, Elmar Böhlen, and Robert Bau*

Contribution from the Department of Chemistry, University of Southern California, Los Angeles, California 90089. Received September 17, 1984

Abstract: Following an earlier report of ours on the preparation and structure determination of the [Cu₅Ph₆]⁻ cluster, we have extended this chemistry into silver/phenyl complexes. The [Ag₃Li₂Ph₆]⁻ mixed-metal cluster was prepared by treating a cold suspension (0 °C) of AgBr in diethyl ether with a solution of freshly prepared phenyllithium in a 1:3 molar ratio. After removal of half of the solvent, large colorless crystals of the title compound appeared after a few days at −15 °C. [Li₆Br₄-(Et₂O)₁₀]²⁺[Ag₃Li₂Ph₆]⁻₂ crystallizes in the monoclinic space group $P2_1/n$, with $a = 16.466$ (9) Å, $b = 29.700$ (15) Å, $c = 12.821$ (5) Å, $\beta = 100.18$ (4)°, $V = 6171$ (5) Å³, $Z = 2$. The positions of the Ag and Br atoms were determined by direct methods, and the coordinates of the rest of the atoms were determined by standard heavy-atom techniques. Least-squares refinement resulted in a final R factor of 0.070 for 3827 reflections with $I > 3 \sigma(I)$. The [Ag₃Li₂Ph₆]⁻ cluster closely resembles the [Cu₅Ph₆]⁻ cluster mentioned earlier, having the same basic trigonal-bipyramidal geometry with lithium atoms in axial positions. The [Li₆Br₄(Et₂O)₁₀]²⁺ cation is extremely unusual: it consists of a [Li₆Br₄]²⁺ salt-like core surrounded by a shell of ten ether molecules.

Organocopper complexes have been used in organic synthesis for many years.[1] This interest has been extended to organosilver compounds for its possible use in organic synthesis[2] as well as its ability to provide some insight into the chemistry of group 11 elements in general. As an extension of our studies on the phenylcopper system,[3] phenylsilver complexes have been investigated.

This paper describes the preparation and structure of one such complex, the [Ag₃Li₂Ph₆]⁻ anion.

The susceptibility of the silver–carbon bond to oxidation and hydrolysis has hindered many early attempts at isolating and characterizing arylsilver compounds.[4] It was only in 1972 that

(1) Posner, G. H. "An Introduction to Synthesis Using Organocopper Reagents"; Wiley: New York, 1980; Chapter 1.
(2) Westmijze, H.; Kleijn, H.; Vermeer, P. *J. Organomet. Chem.* **1979**, *172*, 377.

(3) Edwards, P. G.; Gellert, R. W.; Marks, M. W.; Bau, R. *J. Am. Chem. Soc.* **1982**, *104*, 2072.
(4) (a) Krause, E.; Schmitz, M. *Chem. Ber.* **1919**, *52*, 2159. (b) Krause, E.; Wendt, B. *Chem. Ber.* **1923**, *56*, 2064. (c) Reich, R. *C. R. Hebd. Seances Acad. Sci.* **1923**, *177*, 322.